J Mol Model (2011) 17:2927–2937
DOI 10.1007/s00894-011-0959-x

ORIGINAL PAPER

Computational design and structure–property relationship studies on heptazines

Vikas D. Ghule · Radhakrishnan Sarangapani · Pandurang M. Jadhav · Raj Kishore Pandey

Received: 14 November 2010 / Accepted: 4 January 2011 / Published online: 12 February 2011

Abstract This study aimed to design novel nitrogen-rich heptazine derivatives as high energy density materials (HEDM) by exploiting systematic structure–property relationships. Molecular structures with diverse energetic substituents at varying positions in the basic heptazine ring were designed. Density functional techniques were used for prediction of gas phase heat of formation by employing an isodesmic approach, while crystal density was assessed by packing calculations. The results reveal that nitro derivatives of heptazine possess a high heat of formation and further enhancement was achieved by the substitution of nitro heterocycles. The crystal packing density of the designed compounds varied from 1.8 to 2 g cm^{-3}, and hence, of all the designed molecules, nitro derivatives of heptazine exhibit better energetic performance characteristics in terms of detonation velocity and pressure. The calculated band gap of the designed molecules was analyzed to establish sensitivity correlations, and the results reveal that, in general, amino derivatives possess better insensitivity characteristics. The overall performance of the designed compounds was moderate, and such compounds may find potential applications in gas generators and smoke-free pyrotechnic fuels as they are rich in nitrogen content.

V. D. Ghule
Advanced Center of Research in High Energy Materials (ACRHEM), University of Hyderabad, Hyderabad 500 046, India

R. Sarangapani (✉) · P. M. Jadhav (✉) · R. K. Pandey
High Energy Materials Research Laboratory (HEMRL), Pune 411 021, India
e-mail: sradha78@yahoo.com
e-mail: jadhav.pm@hemrl.drdo.in

Keywords Heptazine · Density functional theory · Isodesmic reaction · Packing calculation · High energy density material

Introduction

High nitrogen content heterocycles have attracted considerable interest as high energy density materials (HEDM) [1–4]. This novel high-nitrogen compounds form a unique class of energetic materials possessing high positive heat of formation (ΔH_f^0) and high thermal stability that result in numerous applications, such as effective precursors of carbon nanospheres and carbon nitride nanomaterials, and as solid fuels in micropropulsion systems, gas generators and smoke-free pyrotechnic fuels [5]. Most of the energy comes either from oxidation of the carbon backbone, as traditionally found in explosives, or from their high nitrogen content.

Over the past few years, 1,3,5-triazine (s-triazine) has played a key role in the molecular routes to carbon nitride (CN_x) materials that have been investigated by various researchers [6–12]. s-Triazine derivatives have been used in the manufacture of polymers, dyes, pesticides and explosives. The s-heptazine structure was first postulated by Pauling and Sturdivant [13] as a component of the polymer melon $[–C_6H_7(NH_2)–NH–]_n$. Such s-triazine monocyclic systems have been subjected to theoretical and experimental studies. Recently, Zheng et al. [14] studied the electronic structure of 1,3,4,6,7,9,9b-heptaazaphenalenes by density functional theory (DFT). Studies on the geometry of heptaazaphenalene derivatives revealed that they have a highly symmetrical structure with a planar and rigid hetero ring. Further, they confirmed the existence of considerable conjugation over the parent ring, which is an advantage in terms of the stability of these compounds. Kroke et al. [15]

reported the synthesis and detailed structural characterization of functionalized 1,3,4,6,7,9,9b-heptaazaphenalene derivatives and 2,5,8-trichloro-1,3,4,6,7,9,9b-heptaazaphenalene. Similar to their s-triazine counterparts, s-heptazine-based precursors are thermally robust candidates as promising precursors to nitrogen-rich, sp^2-bonded carbon nitride materials. Hence, this class of nitrogen-rich molecular system is expected to possess excellent energetic characteristics and may find applications as a high energy material. Molecular frameworks of s-heptazine and s-triazine are represented in Fig. 1.

The key properties of energetic materials in relation to their electronic structure are heat of formation (ΔH_f^0), density (ρ_o), detonation velocity (D), pressure (P), and sensitivity. It is impractical to measure ΔH_f^0 for thermally unstable molecules and new energetic materials for which synthesis is difficult. There are several methods that can predict gas phase ΔH_f^0 from quantum mechanical calculations. DFT methods require less time and computer resources [16, 17] the B3LYP hybrid model in particular can produce reliable geometries and energies. Similarly, density is widely predicted by crystal structure packing calculations, as this method is superior to group additive approaches [18]. The most important explosive performance characteristics, viz., detonation velocity and pressure, were evaluated by Kamlet-Jacobs empirical relations from their theoretical densities and calculated ΔH_f^0 values [19].

Nucleus independent chemical shift (NICS) was defined by Schleyer et al. [20–23] as the negative value of the absolute magnetic shielding computed in ring centers or 1 Å above the molecular plane. NICS may be a useful indicator of aromaticity, which usually correlates well with energetic, structural and magnetic criteria. Negative NICS values denote aromaticity (e.g., −11.5 ppm for benzene and −11.4 ppm for naphthalene) and positive NICS values denote anti-aromaticity (e.g., 28.8 ppm for cyclobutadiene), while small NICS values indicate non-aromaticity (e.g., −2.1 ppm for cyclohexane, −1.1 ppm for adamantane). In principle, no reference molecules or calibrating equations are required for evaluation of aromaticity [24]. In the present study, NICS of the heptazine derivatives in the gas phase were predicted using DFT involving the gauge invariant atomic orbitals (GIAO) method for analyzing the relative stability of the designed molecules.

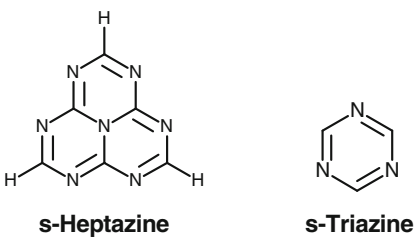

Fig. 1 Molecular frameworks of s-heptazine and s-triazine

Sensitivity prediction has significant importance in deriving novel energetic molecules in terms of their safe handling. Among various aspects of sensitivity, impact sensitivity is measured by a drop weight test and experimental determination associated with large errors. Several simple relationships have been found that relate impact sensitivities with measured and predicted molecular properties, particularly within chemical families [25, 26]. There have been numerous attempts to correlate measured impact sensitivities and various molecular and crystal features; these have included the strengths of certain bonds, NMR chemical shifts, heats of fusion and sublimation, atomic charges, electronic energy levels, the efficiency of lattice-to-molecular vibrational energy transfer, molecular stoichiometry, etc. These efforts, which have often been quite successful, are summarized in more detail elsewhere [27–30]. Politzer et al. [31, 32] considered the surface potential imbalance due to nitro groups as symptomatic of sensitivity. The trigger linkage concept is that a key step in the initiation of detonation is the rupture of a specific type of bond. C–NO_2, O–NO_2 and N–NO_2 are presumed trigger bonds, and their rupture is a dominant factor in determining sensitivity. Recently, Xu et al. [33] analyzed the relationship between impact sensitivities and electronic structures of some nitro compounds. Kunz et al. [34–37] predicted the band gap of organic and inorganic materials using the Hartree-Fock approximation based on their electronic structures. Analysis of the band gap between highest occupied molecular orbital (HOMO) and lowest unoccupied molecular orbital (LUMO) has been suggested relative to the sensitivity of the material [38]. The present study explores sensitivity relationships by analyzing band gap.

The present study aims to design novel nitrogen-rich heptazine derivatives for energetic material applications by exploiting systematic structure–property relationships. DFT was used for the prediction of ΔH_f^0 by employing an isodesmic approach. Crystal density was predicted by forcefield-based packing calculations. Energetic groups like nitro and azido, and nitrogen-rich heterocycles (imidazloes, triazoles etc.) proved to enhance the energetic behavior of the explosive. Hence, molecular structures with diverse substituents, viz. azido, amino, nitro, and nitrogen-rich heterocycles, at various positions in the basic s-heptazine ring were considered; the structures of the compounds considered are shown in Fig. 2.

Theoretical methodology

Quantum-chemical calculations were performed with the Gaussian 03 package [39]. The Becke three-parameter hybrid functional was used along with Lee-Yang-Parr

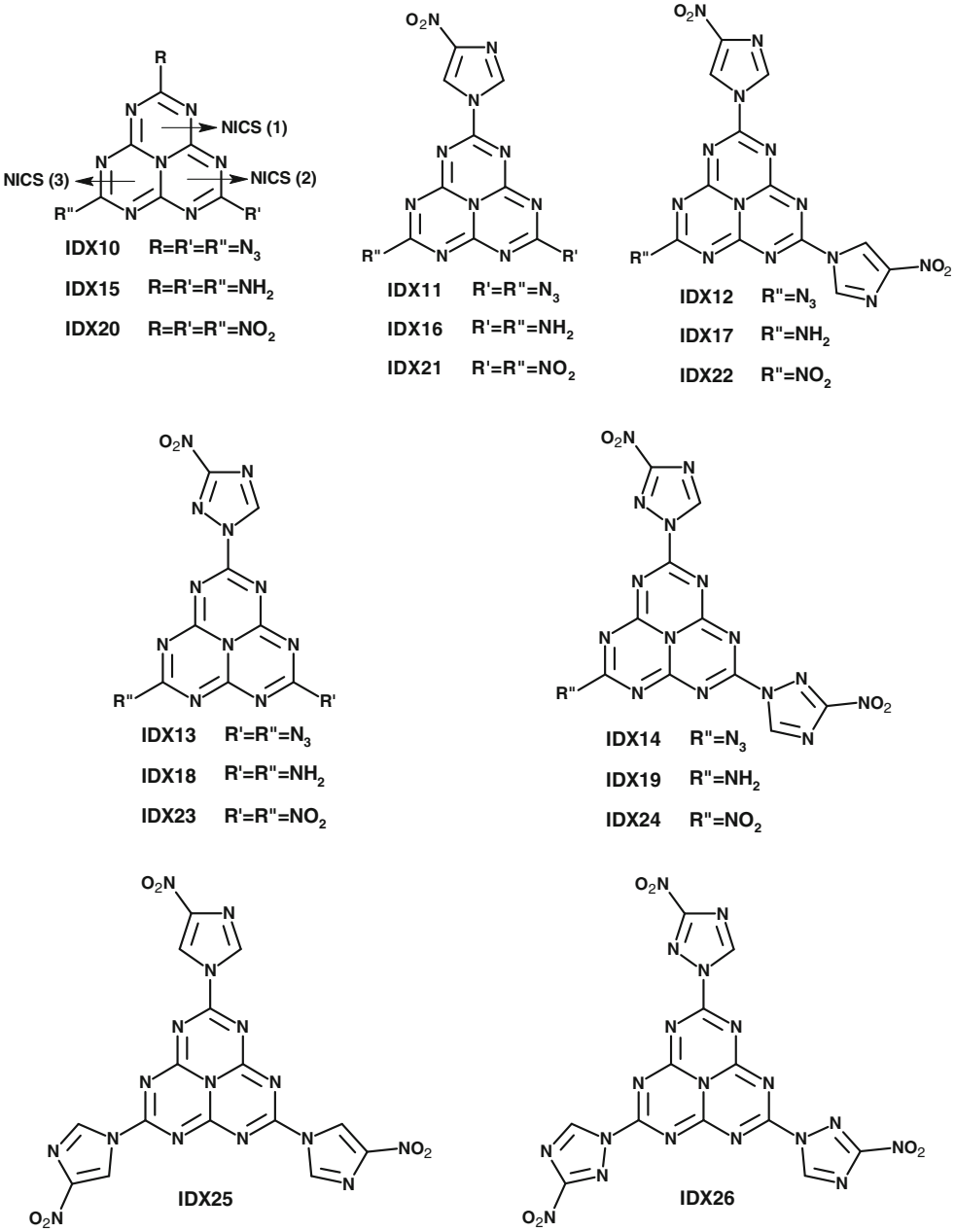

Fig. 2 Designed heptazine derivatives (substituted groups on the ring represented as R, R′, and R″). Nucleus independent chemical shift (NICS) (1), NICS (2), and NICS (3) represent the contributions of individual ring centers

(LYP) correlation [40–42]. The 6-31G* basis set was employed for all optimization and harmonic vibrational frequency calculations, [43]. The density of the crystal structure of all the designed molecules was predicted by rigorous molecular packing calculations using the polymorph module of the Material Studio Suite [44]. Dreiding [45] force field was employed for calculations with different space groups. The approach is based on the generation of possible packing arrangements in all reasonable space groups ($P2_1/c$, P−1, $P2_12_12_1$, C_2/c, $P2_1$, Pbca, $Pna2_1$, Cc, Pbcn and C_2) to search for low-lying minima in the lattice energy surface [46–48].

The empirical Kamlet-Jacobs [19] equations were employed to estimate the values of D and P for high energy materials containing C, H, O and N as follows:

$$D = 1.01\left(NM^{1/2}Q^{1/2}\right)^{1/2}(1 + 1.30\rho_o) \quad (1)$$

$$P = 1.55\rho_o{}^2NM^{1/2}Q^{1/2} \quad (2)$$

Where, D is detonation velocity (km s^{-1}), P is detonation pressure (GPa), N is moles of gaseous detonation products

Table 1 Total energy (E_0) at 298K and gas phase ΔH_f^0 for the reference compounds at the B3LYP/6-31G* level

Compound	E_0 (au)	ΔH_f^0	
		kJ/mol	cal/g
CH_4	-40.46935	-74.8	-1,117.35
NH_3	-56.50961	-45.9	-645.32
CH_3NH_2	-95.78443	-22.5	-173.19
CH_3NO_2	-244.95385	-74.7	-292.49
CH_3N_3	-204.03725	238.5	999.17
$(CH_3)_3N$	-174.46792	-23.7	-95.83
Imidazole	-226.20972	129.5	454.63
1H-1,2,4-triazole	-242.24467	192.7	666.90
s-Triazine	-280.35961	225.8	665.69

per gram of explosive, M is average molecular weights of gaseous products, Q is chemical energy of detonation (kJ mol^{-1}) defined as the difference of ΔH_f^0 between products and reactants, and ρ_o is the density of explosive (g cm^{-3}).

NICS of different derivatives of the heptazines in gas phase were predicted using the GIAO method. B3LYP/6-31G* calculation was employed to predict NICS at ring centers. NICS values of the individual rings of s-heptazine are represented as NICS-1, NICS-2 and NICS-3 in Fig. 2.

Results and discussion

Recently, Gillan et al. [49] demonstrated a synthetic route for heptazine and 2,5,8-triazido-s-heptazine (Fig. 2). They also indicated that these compounds can act as potential energetic materials. Strout et al. [50–52] studied the nitrogen-rich molecules by theoretical calculations to predict their energetic properties as high energy density materials. This paper focuses on a study of electronic structure and its effect on thermodynamic and energetic characteristics using density functional techniques.

Heat of formation

Heat of formation (ΔH_f^0) is one of the most important thermo-chemical properties of energetic materials because it is related directly with detonation parameters. All heat of formation data are in cal g^{-1} as well as kJ mol^{-1}, since the formulas for detonation velocity and detonation pressure dictate that the energy produced in decomposition or combustion be given on a gram basis [53–56]. The zero point energies and thermal correction for model compounds have been calculated at the B3LYP/6-31G* level. ΔH_f^0 of model compounds has been predicted using B3LYP method in combination with the 6-31G* basis set through appropriate design of isodesmic reactions [57]. The isodesmic reaction, in which a number of electron pairs and chemical

Table 2 Calculated energetic properties of designed heptazine derivatives. *NC* Nitrogen content, ΔH_f^0 heat of formation, Q chemical energy of detonation, D detonation velocity, P pressure

Compound	NC (%)	ΔH_f^0		Q (cal/g)	N (mol/g)	M (g/mol)	D (km/s)	P (GPa)
		kJ/mol	cal/g					
H	56.65	811.99	1,121.79	1,121.79	0.029	20.20	6.68	18.90
IDX10	75.67	1,187.29	958.68	958.68	0.027	28.00	7.10	22.35
IDX11	61.20	1,340.16	875.15	1,105.23	0.027	27.00	7.50	25.44
IDX12	51.37	1,497.39	820.84	1,207.11	0.027	26.33	7.56	25.60
IDX13	64.84	1,418.59	923.85	1,110.55	0.028	27.52	7.81	27.84
IDX14	57.53	1,656.55	903.94	1,216.82	0.029	27.23	8.05	29.43
IDX15	64.20	761.69	835.08	835.08	0.037	18.25	7.46	25.48
IDX16	53.49	1,026.61	781.42	1,149.52	0.028	22.89	7.39	24.52
IDX17	47.80	1,334.84	778.13	1,265.43	0.027	25.27	7.50	25.31
IDX18	57.77	1,105.02	838.42	1,205.36	0.028	24.33	7.64	26.37
IDX19	54.36	1,491.25	865.09	1,273.87	0.029	26.33	7.94	28.45
IDX20	45.46	891.82	692.04	1,206.67	0.036	28.00	9.25	40.10
IDX21	44.92	1,225.85	783.38	1,291.08	0.032	27.17	8.49	32.74
IDX22	44.54	1,397.95	759.36	1,262.21	0.029	26.46	7.93	28.17
IDX23	48.53	1,383.55	881.81	1,346.31	0.034	27.60	8.95	36.90
IDX24	50.68	1,563.17	845.26	1,274.85	0.032	27.29	8.49	32.48
IDX25	44.26	1,658.26	783.27	1,282.53	0.028	25.86	7.54	25.15
IDX26	52.26	1,898.24	891.33	1,295.20	0.031	27.03	8.12	29.41

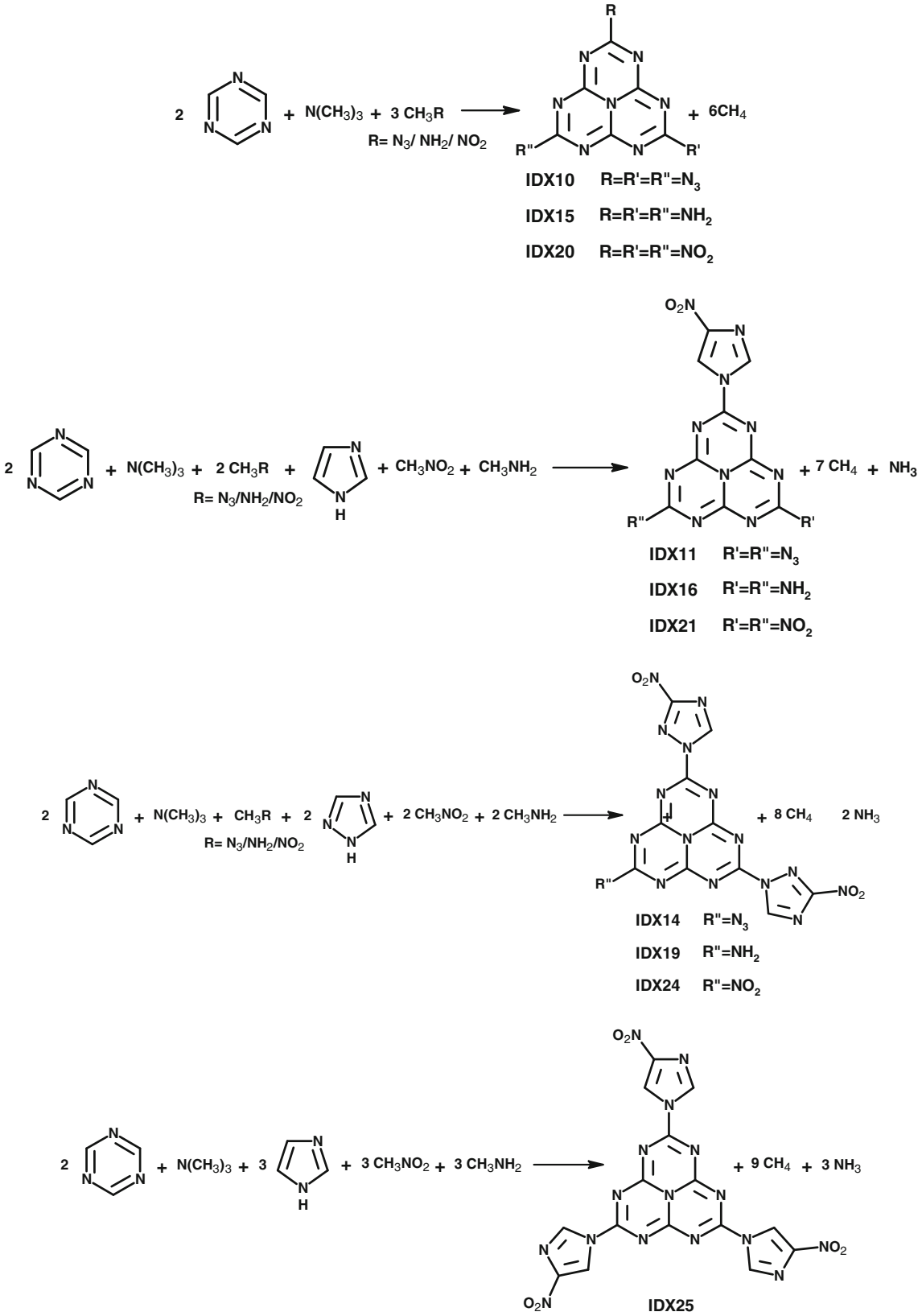

Fig. 3 Isodesmic reaction schemes for the designed molecules

bond types are conserved in the reaction [58], allows canceling of errors inherent in the approximate treatment of the electron correlation in the solutions to quantum mechanic equations. In addition, reasonably accurate predictions of ΔH_f^0 are possible by utilizing isodesmic schemes, even at relatively low levels of theory. However, good experimental values must be available for all but one reaction component, and it is also known that different isodesmic reactions will predict different values for the same component [59]. Recently, the isodesmic reaction approach has been used for determination of ΔH_f^0 within a few kcal mol^{-1} of deviations from experimental values [60]. The calculated and experimental gas phase ΔH_f^0 of the reference compounds [61–64] s-triazine, imidazole, 1,2,4-triazole, CH_4, NH_3, CH_3N_3, CH_3NO_2, CH_3NH_2 are listed in Table 1. The ΔH_f^0 of title compounds predicted by the isodesmic approach are summarized in Table 2. All the predicted molecules show that high positive ΔH_f^0 may be due to high nitrogen content, conjugation, planarity, stability of structure based on s-triazine and the large number of inherently energetic N–N and C–N bonds.

Figure 3 shows the isodesmic reaction schemes for the designed molecules and calculated ΔH_f^0 of the parent s-heptazine (**H**) by a similar reaction at about 812 kJ mol^{-1}. Comparison of **IDX10**, **IDX20** with the parent heptazine ring clearly indicates that introduction of explosophores like azido, nitro etc., increases the ΔH_f^0 of the parent system. This proves that azido and nitro explosophores are the main origin of the energy center in the designed molecules. The role of the azido group in heat of formation is more profound than that of the nitro group, as also found by Li et al. [38]. This may be attributed to the higher nitrogen content of **IDX10**; however, introduction of a nitro group enhances the oxygen balance and hence the overall performance. Introduction of an amino group (**IDX15**) brings down the ΔH_f^0 , as supported by Li et al. [38, 65].

Imidazole and triazole are natural frameworks for energetic materials as they have inherently high nitrogen content [66]. Introduction of an amino group is one of the simplest means to enhance the thermal stability of an energetic material [67]. Adding these functionalities to the ring structure typically alters the ΔH_f^0 , making it more positive—a desired characteristic for most energetic materials [4]. A systematic substitution of nitro, azido and amino groups by imidazole and triazole was attempted in order to design a novel high energy material with optimal performance characteristics. Substitution by imidazole or 1H-1,2,4-triazole with a nitro group shows a remarkable increase in ΔH_f^0; various s-heptazine derivatives are compared in Figs. 4 and 5, indicating that addition of nitrogen heterocycle increases the ΔH_f^0. Replacement of the azido group in **IDX10** by nitroimidazole (in **IDX11** and **IDX12**) and nitrotriazole (in **IDX13** and **IDX14**) increases

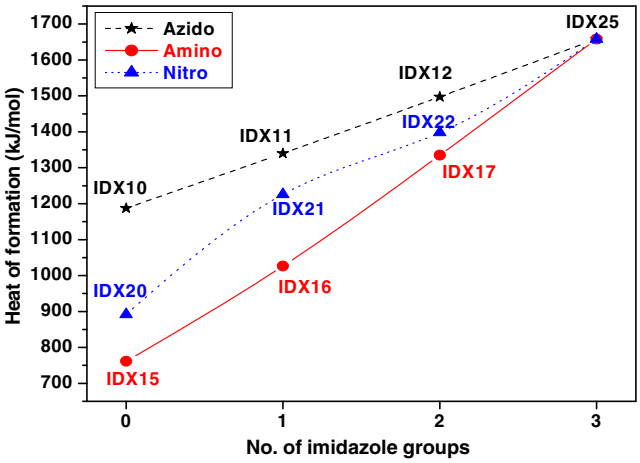

Fig. 4 Plot of number of imidazole groups versus heat of formation (kJ mol^{-1})

the ΔH_f^0 significantly, which indicates that corresponding rings contribute significantly to the total ΔH_f^0 of the molecules. The energy contribution to the overall gas phase ΔH_f^0 of imidazole (129.5 kJ mol^{-1}) is lower than triazole ring (192.7 kJ mol^{-1}). This can be clearly seen in **IDX11** and **IDX13**, in which ΔH_f^0 is increased by 78 kJ mol^{-1} and in **IDX12** and **IDX14** ΔH_f^0 is increased by 159 kJ mol^{-1}. A similar trend is observed in the case of amino (**IDX16** to **IDX18** by 79 kJ mol^{-1}; **IDX17** to **IDX19** by 157 kJ mol^{-1} and nitro derivatives (**IDX21** to **IDX23** by 158 kJ mol^{-1}; **IDX22** to **IDX24** by 166 kJ mol^{-1}). Overall, tri-substituted **IDX25** and **IDX26** is calculated to have high gas phase ΔH_f^0 viz., 1,658.26 and 1,898.24 kJ mol^{-1}, respectively. Comparison of **IDX11**, **IDX16** and **IDX21**, in which one of the functional groups (azido, amino and nitro) is replaced by a nitroimidazole group shows the following order of ΔH_f^0 **IDX11**>**IDX21**>**IDX16**. Similarly, in the case of the nitro triazole substitution, the order is **IDX13**>**IDX23**>**IDX18**, which indicates that azido and nitro deriva-

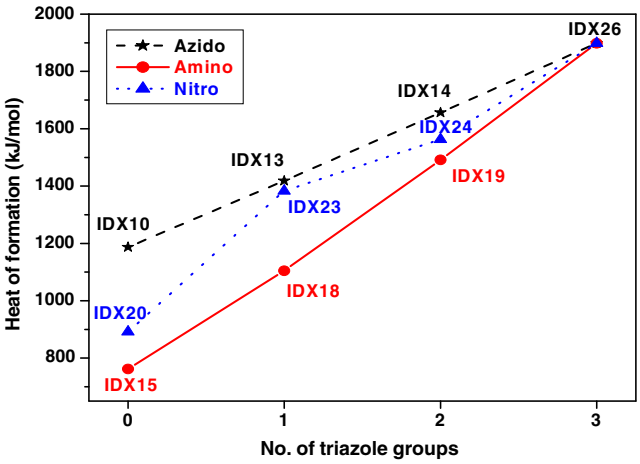

Fig. 5 Plot of number of triazole groups versus heat of formation (kJ mol^{-1})

tives exhibit higher ΔH_f^0 than amino functionalization. In the case of diheterocyclic-substituted compounds, a similar order is found, viz., **IDX12**>**IDX22**>**IDX17** and **IDX14**>**IDX24**>**IDX19**. Overall, nitro heterocycle substitution increases the ΔH_f^0 , and energy contribution from the triazole ring is higher than that from the imidazole ring.

Density

Density is an important parameter of explosives in detonation performance because detonation velocity and pressure of the explosives increase proportionally with the packing density and square of density, respectively [19]. Density is a condensed phase property and its prediction involves challenges as it is associated with different intermolecular interactions affecting crystal pattern and cell volume. Heterocycles generally have a higher heat of formation, density and oxygen balance than their carbocyclic analogues. In general, possible ways of improving the density are (1) increasing the concentration of nitro groups, which increases the opportunity for hydrogen bonding; (2) making larger compounds; and (3) replacing single bonds with double bonds [68–71]. As bond length decreases, molecular volume is expected to decrease [72]. In the present study, these design principles were used while designing the model compounds and the calculated densities from packing calculations are shown in Table 3.

Introduction of one imidazole and triazole ring increases the density of heptazine viz, 1.80 g cm^{-3} increases the density to 1.86 (**IDX11**) and 1.89 g cm^{-3} (**IDX13**), respectively. However, further introduction of additional heterocyclic ring in **IDX12** and **IDX14** decreases the density to 1.83 and 1.87 g cm^{-3}, respectively, as compared to **IDX11** and **IDX13**. This may be attributed to the increase in molecular volume and the orientation of the ring in space. The density of triaminoheptazine **(IDX15)** is 1.90 g cm^{-3} and results reveal that replacement of the amino group with nitroimidazoles/nitrotriazoles decreases the density. The amino group lies in the same plane of the molecule to maximize lone pair delocalization with the heterocyclic π-electron system, and further helps in increasing hydrogen bonding with nitro groups of the hetero ring.

The symmetrical trinitroheptazine (**IDX20**) possesses a very high density of 1.98 g cm^{-3}, which may be due to the high content of oxygen and nitrogen. Nitro derivatives of heptazines follow a similar trend of amino and azido derivatives when introducing the heterocyclic ring. In the case of **IDX25** and **IDX26**, the molecular volume is very high due to the presence of three nitro substituted heterocyclic rings, and hence the overall density is less. The overall density of the designed molecules varies from 1.8 to 2 g cm^{-3}. Figure 6 shows the representative predicted crystal structures of **IDX12**, **IDX24**, and **IDX25**.

Table 3 Calculated cell parameters and densities of the designed molecules

Compound	Density (g/cm^3)	Space group	Cell volume (Å^3)	Lattice parameters					
				Length (Å)			Angle (degrees)		
				a	b	c	α	β	γ
H	1.67	P1	349.25	14.809	6.862	8.012	106.5	128.0	116.4
IDX10	1.80	P21/c	1,095.36	3.453	23.431	17.149	90.0	165.6	90.0
IDX11	1.86	P1	656.72	10.442	7.647	10.218	77.5	57.0	90.0
IDX12	1.83	P21/c	1,611.54	19.971	18.716	21.879	90.0	168.6	90.0
IDX13	1.89	PBCA	2,580.59	7.058	21.448	17.045	90.0	90.0	90.0
IDX14	1.87	PNA21	1,559.73	18.083	12.233	7.051	90.0	90.0	90.0
IDX15	1.90	P21/c	798.87	9.871	3.730	25.207	90.0	59.4	90.0
IDX16	1.84	C2/c	2,306.53	69.368	4.311	52.195	90.0	171.5	90.0
IDX17	1.83	P1	752.58	12.230	15.812	4.865	123.0	78.6	85.2
IDX18	1.86	P21/c	1,142.30	8.960	33.024	33.708	90.0	173.5	90.0
IDX19	1.85	P1	748.20	11.527	11.829	11.533	138.5	46.7	116.1
IDX20	1.98	Cc	1,033.71	3.472	31.563	10.782	90.0	61.0	90.0
IDX21	1.87	P1	667.37	18.001	7.941	13.326	54.1	145.7	140.9
IDX22	1.83	P21/c	1,613.94	4.109	16.389	25.698	90.0	68.8	90.0
IDX23	1.92	P21/c	1,298.42	15.676	9.774	8.598	90.0	99.7	90.0
IDX24	1.89	PBCA	3,115.36	7.682	22.384	18.116	90.0	90.0	90.0
IDX25	1.79	P21	946.57	4.258	12.745	21.637	90.0	126.3	90.0
IDX26	1.82	PBCA	3,735.80	35.615	7.388	14.197	90.0	90.0	90.0

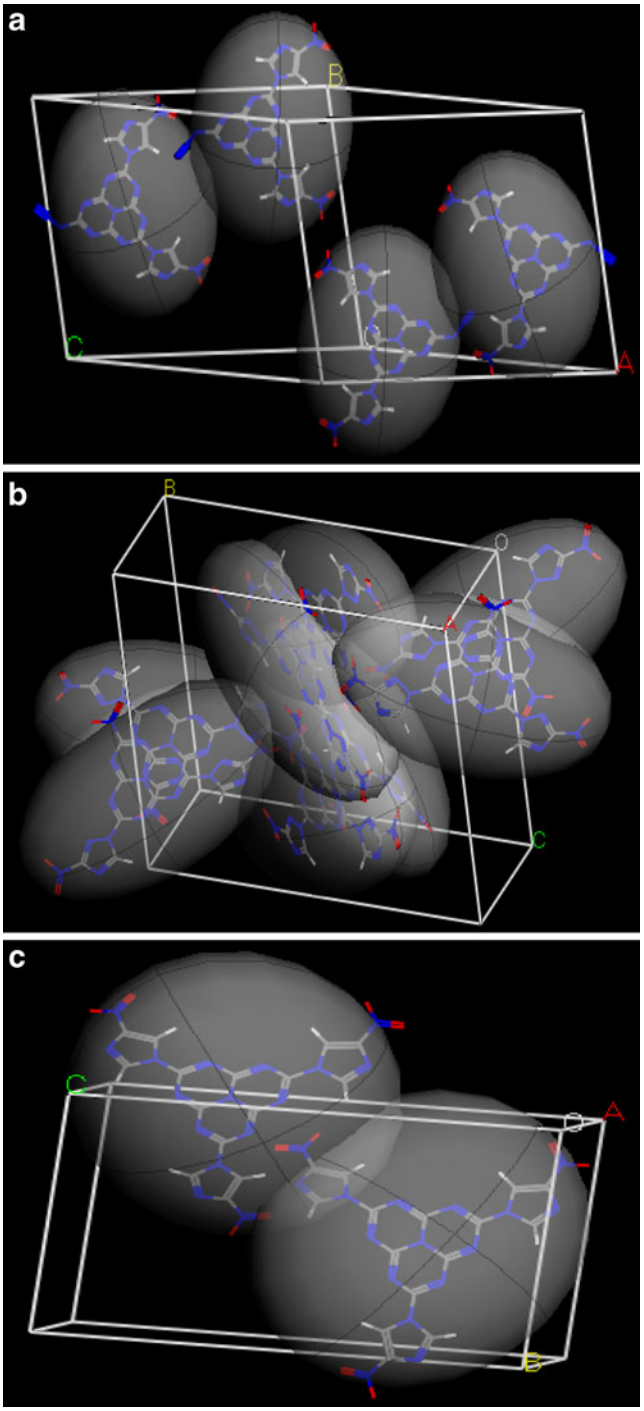

Fig. 6 Predicted crystal structures of **a** **IDX12**, **b** **IDX24** and **c** **IDX25**

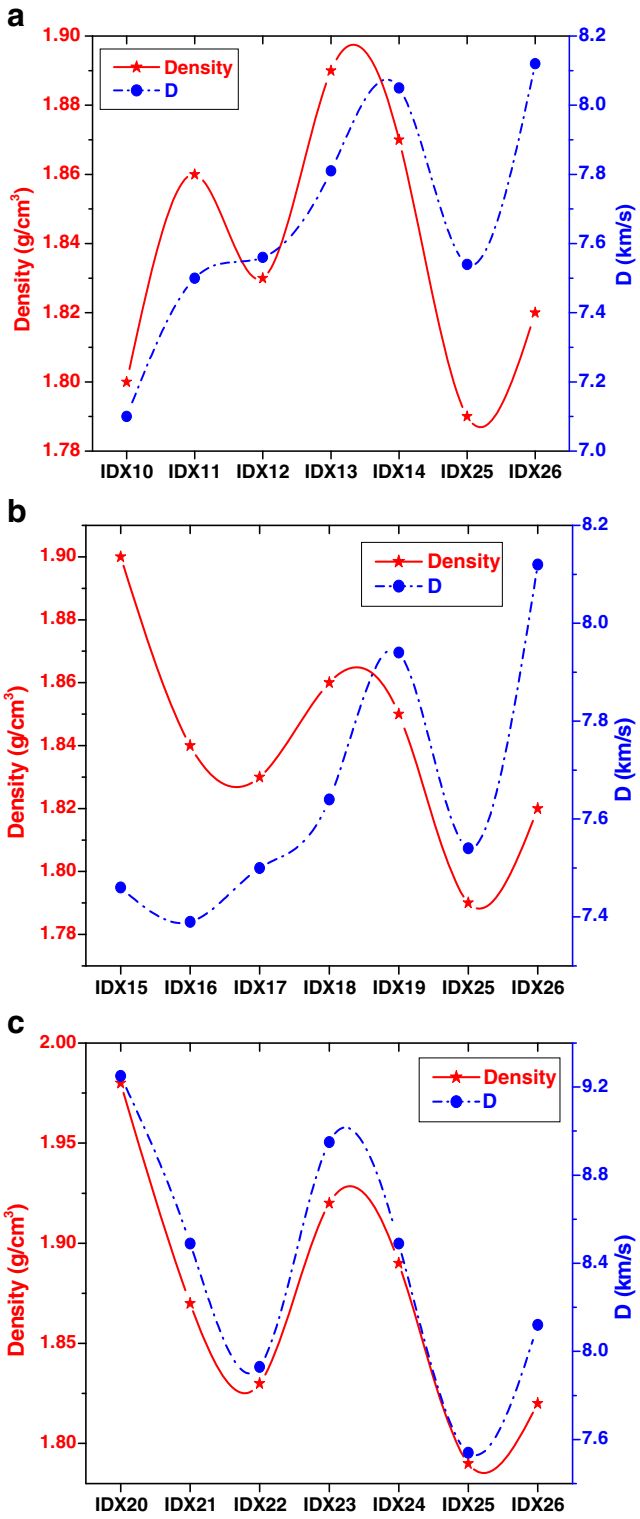

Fig. 7 Density and detonation velocity (D) profiles of **a** azide derivatives, **b** amino derivatives, and **c** nitro derivatives of heptazine

Detonation performance

Table 2 represents detonation velocity and pressure for the predicted molecules computed by Kamlet-Jacobs empirical equations. Overall computed detonation velocity ranges from about 7.1 to 9.3 km s^{-1}, and oxygen balance is negative in all cases. Figure 7a–c shows the dependence on density of the detonation velocity and clearly indicates that nitrotriazole-substituted derivatives show overall high detonation velocity. Cho et al. [73] also reported that the performance of an explosive is highly sensitive to its

crystalline density, but somewhat less sensitive to its ΔH_f^0. Comparison of azido derivative reveals the order of detonation performance as **IDX14**>**IDX13**>**IDX12**>**IDX11**>**IDX10**. Replacement of azido groups with nitroimidazole and nitrotriazole groups enhances the detonation performance of the molecules due to higher densities and greater mole of gaseous detonation products per gram of explosive (N).

In the case of amino derivatives, **IDX16** exhibits a lower performance than its parent molecule **IDX15** even after an energetic nitroimidazole group is introduced. Performance reduction can be attributed to the decrease in density. Comparison of amino derivatives reveals that these compounds (**IDX17**, **IDX18** and **IDX19**) have low density as compared to **IDX15**. However, ΔH_f^0 of these compounds is very high. The order of the detonation performance for the amino series derivatives can be given as **IDX16**<**IDX15**<**IDX17**<**IDX18**<**IDX19**. In general, these derivatives exhibit about 7.6 km s^{-1} detonation velocity, and 25.5 GPa detonation pressure. The number of moles of gaseous detonation products per gram of explosive (N) is less due to the low oxygen balance in these amino derivatives.

Nitro derivatives of heptazines (**IDX20**, **IDX21**, **IDX22**, **IDX23**, and **IDX24**) show higher performance than azido and amino derivatives due to better oxygen balance, density and ΔH_f^0 of these molecules. Molecules **IDX21** and **IDX22** possess lower densities than the parent **IDX20**, which results in poorer performance than **IDX20**. **IDX23** and **IDX24** show comparable performance to **IDX20**. Detonation performance increases as the moles of gaseous detonation products per gram of explosive increases. Among the nitro derivatives, **IDX20** possess a high detonation velocity of 9.25 km s^{-1}, while other derivatives exhibit a detonation velocity of about 8 km sec^{-1} and detonation pressure of 35 GPa. Their order of their detonation performance can be given as **IDX22**<**IDX24**<**IDX21**<**IDX23**<**IDX20**. The designed molecules **IDX25** and **IDX26** have higher ΔH_f^0 but poor densities. Further **IDX25** has low moles of gaseous detonation products per gram of explosive as compared to **IDX26**, which results in **IDX26** being superior to **IDX25**.

Stability and sensitivity correlations

NICS is expressed by a combination of properties in cyclic delocalized systems and can be discussed in terms of energetic, structural and magnetic criteria. Negative values of NICS indicate the shielding presence of induced diatropic ring currents that are understood as aromaticity at specific points [10]; the more negative the NICS, the more aromatic the rings. Further, cyclic electron delocalization results in enhanced stability, bond length equalization, and special magnetic as well as chemical and physical properties [74–76]. The NICS value for the parent

Table 4 Calculated nucleus independent chemical shift (NICS) and band gap of the designed molecules. *HOMO* Highest occupied molecular orbital, *LUMO* lowest unoccupied molecular orbital

Compound	NICS(1) ppm[a]	NICS(2) ppm	NICS(3) ppm	E_{HOMO} (Hartree)	E_{LUMO} (Hartree)	ΔE(Hartree)
H	4.84	4.83	4.85	-0.2596	-0.1162	0.1434
IDX10	1.45	1.46	1.45	-0.2661	-0.1156	0.1504
IDX11	1.48	2.18	1.42	-0.2777	-0.1315	0.1462
IDX12	1.48	2.17	2.18	-0.2870	-0.1460	0.1410
IDX13	1.62	2.22	1.65	-0.2820	-0.1339	0.1480
IDX14	1.68	2.41	2.39	-0.2976	-0.1508	0.1468
IDX15	0.09	0.80	0.79	-0.2213	-0.0388	0.1824
IDX16	-0.02	0.17	-0.01	-0.2546	-0.0941	0.1605
IDX17	1.45	1.79	1.79	-0.2786	-0.1286	0.1499
IDX18	1.15	1. 48	1.20	-0.2555	-0.1015	0.1540
IDX19	1.61	1.97	1.97	-0.2860	-0.1348	0.1511
IDX20	2.75	2.72	2.73	-0.3178	-0.1764	0.1414
IDX21	-1.85	2.35	-1.74	-0.2980	-0.1617	0.1362
IDX22	1.44	2.57	2.57	-0.2927	-0.1573	0.1353
IDX23	2.07	3.41	2.18	-0.3134	-0.1689	0.1444
IDX24	1.59	2.96	2.96	-0.3147	-0.1714	0.1433
IDX25	2.23	2.34	2.23	-0.2962	-0.1614	0.1347
IDX26	2.49	2.69	2.58	-0.3107	-0.1677	0.1429

[a] NICS(1), NICS(2) and NICS(3) represent values for individual rings in s-heptazine as shown in Fig. 1

s-heptazine ring is found to be 4.84 ppm, while for the designed molecules the values are calculated to be less than those of the parent molecule. This indicates that substitution brings stability in the compounds due to the electronic effects of substitution (azido, amino and nitro, imidazole and triazole groups). The diatropic current of the ring increases due to substituted groups and the electrons are expected to be located mainly on the nitrogen atoms due to their high electronegativity compared to the carbon atom. Comparison of **H**, **IDX10**, **IDX15** and **IDX20** reveals that the profound electron donating effect of the amino group increases the ring current strongly, which leads to lower values of NICS. Further, the symmetric arrangement of the azido (**IDX10**), amino (**IDX15**) and nitro (**IDX20**) groups increases stability through delocalization of π-electrons, thus enhancing cyclic conjugation; accordingly, their order of stability is **IDX15**>**IDX10**>**IDX20**>**H**. Substitution of the nitro imidazole group on **IDX11**, **IDX16**, and **IDX21** shows an increase in NICS (2) at the corresponding ring of the heptazine, which may be due to its own contribution towards aromaticity; the same trend has been found in the case of triazole compounds. In tri-heterocycle-substituted molecules, **IDX25** shows better stabilization than **IDX26**, this can be attributed to the better contribution of the imidazole ring compared to triazole.

The band gap between the HOMO and LUMO has been suggested to be a measure of the sensitivity of the material [33, 38]. In principle, the band gap (ΔE) between HOMO and LUMO is used as a criterion to predict the sensitivity of the material; the smaller the ΔE, easier the electron transits and the larger the sensitivity. The band gap of predicted heptazine derivatives obtained using B3LYP/6-31G* method is compiled in Table 4. It is well known that the introduction of an amino group into polynitrobenzenes can increase stability under stimuli of impact and shock [77, 78]. From the ΔE values of the heptazine derivatives, it can be seen that molecule **IDX15** possess a high band gap of 0.18 Hartree, which indicates that **IDX15** will be relatively more insensitive than the designed molecules. Comparison of **IDX10**, **IDX15** and **IDX20** reveals that trinitro derivatives are more sensitive than azido and amino derivatives. Replacement of the amino group with other heterocycles increase the sensitivity as seen in **IDX16**, **IDX17**, **IDX18**, **IDX19**, **IDX25** and **IDX26**. A similar trend is observed in azido and nitro derivatives. Comparison of **IDX25** and **IDX26** indicates that nitro triazole has better insensitivity characteristics than nitro imidazole. Nitro derivatives of heptazines possess better energetic performance characteristics than others. However, NICS analysis and insensitivity correlations revealed that amino derivatives are better candidates considering insensitivity and stability.

Conclusions

Molecular structures with diverse energetic substituents at varying positions in the basic heptazine ring have been designed for HEM applications. DFT techniques were used to predict gas phase heats of formation using an isodesmic approach, while crystal density was determined by packing calculations. Among the designed molecules, nitro derivatives of heptazine exhibited the best performance characteristics, while amino derivatives are better in terms of insensitivity and stability. Although the designed molecules are not superior to reported HEMs, these molecules may find potential applications in gas generators and smoke-free pyrotechnic fuels as they are rich in nitrogen content. In addition, the study finds its usefulness in realizing structure–property correlations.

Acknowledgments The authors thank Dr. A. Subhananda Rao, Director and Mr. B. Bhattacharya, Associate Director, HEMRL, for their approval to publish this work. The authors also thank Prof. S. P. Tewari and Prof. M. Durga Prasad, University of Hyderabad, for useful discussions and support. V.D.G. thanks ACRHEM, University of Hyderabad for financial support.

References

1. Hammerl A, Klapotke TM (2002) Inorg Chem 41:906–912
2. Gagliardi L, Pyykko PJ (2001) J Am Chem Soc 123:9700–9701
3. Li YF, Wang ZY, Ju XH, Fan XW (2009) J Mol Struct THEOCHEM 907:29–34
4. Gutowski KE, Rogers RD, Dixon DA (2006) J Phys Chem A 110:11890–11897
5. Xue H, Gao Y, Twamley B, Shreeve JM (2005) Chem Mater 17:191–198
6. Khabashesku VN, Zimmerman JL, Margrave JL (2000) Chem Mater 12:3264–3270
7. Gillan EG (2000) Chem Mater 12:3906–3912
8. Wang J, Miller DR, Gillan EG (2003) Carbon 41:2031–2037
9. Komatsu TJ (2001) J Mater Chem 11:799–801
10. Turker L, Atalar T, Gumus S, Camur Y (2009) J Hazard Mater 167:440–448
11. Ye C, Gard GL, Winter RW, Syvret RG, Twamley B, Shreeve JM (2007) Org Lett 9:3841–3844
12. Huynh MHV, Hiskey MA, Hartline EL, Montoya DP, Gilardi R (2004) Angew Chem Int Ed 43:4924–4928
13. Pauling L, Sturdivant JH (1937) Proc Natl Acad Sci USA 23:615–620
14. Zheng W, Wong N, Wang W, Zhou G, Tian A (2004) J Phys Chem A 108:97–106
15. Kroke E, Schwarz M, Bordon EH, Kroll P, Noll B, Norman AD (2002) New J Chem 26:508–512
16. Parr RG, Yang W (1989) Density functional theory of atoms and molecules. Oxford University Press, Oxford
17. Byrd EFC, Rice BM (2007) J Phys Chem C 111:2787–2796
18. Peralta-Inga Z, Degirmenbasi N, Olgun U, Gocmez H, Kalyon DM (2006) J Energ Mater 24:69–101
19. Kamlet MJ, Jacobs SJ (1968) J Chem Phys 48:23–35
20. Cyranski MK, Krygowski TM, Katritzky AR, PvR S (2002) J Org Chem 67:1333–1338

21. Schleyer PvR, Kiran B, Simion DV, Sorensen TS (2000) J Am Chem Soc 122:510–515
22. Schleyer PvR, Maerker C, Dransfeld A, Jiao H, Eikema Hommes NJR (1996) J Am Chem Soc 118:6317–6318
23. PvR S (2001) Chem Rev 101:1115–1117
24. Zahedi E, Aghaie M, Zare K (2009) J Mol Struct THEOCHEM 905:101–105
25. Cho SG, No KT, Goh EM, Kim JK, Shin JH, Joo YD, Seong S (2005) Bull Korean Chem Soc 26:399–408
26. Badders NR, Wei C, Aldeeb AA, Rogers WJ, Mannan MS (2006) J Energ Mater 24:17–33
27. Brill TB, James K (1993) Chem Rev 93:2667–2692
28. Rice BM, Hare JJ (2002) J Phys Chem A 106:1770–1783
29. Politzer P, Murray JS (2003) Energetic materials, part 2. In: Politzer P, Murray JS (eds) Detonation, combustion. Elsevier, Amsterdam
30. Zeman S (2007) Struct Bond 125:195–271
31. Pospisil M, Vavra P, Concha MC, Murray JS, Politzer P (2010) J Mol Model 16:895–901
32. Murray JS, Concha MC, Politzer P (2009) Mol Phys 107:89–97
33. Xu XJ, Zhu WH, Xiao HM (2007) J Phys Chem B 111:2090–2097
34. Kunz AB (1996) Phys Rev B 53:9733–9738
35. Pandey R, Jaffe JE, Kunz AB (1991) Phys Rev B 43:9228–9237
36. Kuklja MM, Kunz AB (1999) J Phys Chem B 103:8427–8431
37. Kuklja MM (2000) Kunz AB 61:35–44
38. Li YF, Fan XW, Wang ZY, Ju XH (2009) J Mol Struct THEOCHEM 896:96–102
39. Frisch MJ, Trucks GW, Schlegel HB, Scuseria GE, Robb MA, Cheeseman JR, Montgomery JA, Vreven T Jr, Kudin KN, Burant JC, Millam JM, Iyengar SS, Tomasi J, Barone V, Mennucci B, Cossi M, Scalmani G, Rega N, Petersson GA, Nakatsuji H, Hada M, Ehara M, Toyota K, Fukuda R, Hasegawa J, Ishida M, Nakajima T, Honda Y, Kitao O, Nakai H, Klene M, Li X, Knox JE, Hratchian HP, Cross JB, Adamo C, Jaramillo J, Gomperts R, Stratmann RE, Yazyev O, Austin AJ, Cammi R, Pomelli C, Ochterski JW, Ayala PY, Morokuma K, Voth GA, Salvador P, Dannenberg JJ, Zakrzewski VG, Dapprich S, Daniels AD, Strain MC, Farkas O, Malick DK, Rabuck AD, Raghavachari K, Foresman JB, Ortiz JV, Cui Q, Baboul AG, Clifford S, Cioslowski J, Stefanov BB, Liu G, Liashenko A, Piskorz P, Komaromi I, Martin RL, Fox DJ, Keith T, Al-Laham MA, Peng CY, Nanayakkara A, Challacombe M, Gill PM, Johnson B, Chen W, Wong MW, Gonzalez C, Pople JA (2003) Gaussian 03, Revision A.1. Gaussian Inc, Pittsburgh, PA
40. Stephens PJ, Devlin FJ, Chabalowski CF, Frisch MJ (1994) J Phys Chem 98:11623–11627
41. Becke AD (1993) J Chem Phys 98:5648–5652
42. Lee C, Yang W, Parr RG (1988) Phys Rev B 37:785–789
43. Rassolov VA, Ratner MA, Pople JA, Redfern PC, Curtiss LA (2001) J Comput Chem 22:976–984
44. Materials Studio 4.01 (2004) Accelrys Inc., San Diego, CA
45. Mayo SL, Olafson BD, Goddard WA (1990) J Phys Chem 94:8897–8909
46. Baur WH, Kassner D (1992) Acta Crystallogr Sect B 48:356–369
47. Belsky VK, Zorkii PM (1977) Acta Crystallogr Sect A 33:1004–1006
48. Xu XJ, Zhu WH, Gong XD, Xiao HM (2008) Sci China Ser B-Chem 51:427–439
49. Miller DR, Swenson DC, Gillan EG (2004) J Am Chem Soc 126:5372–5373
50. Strout DL (2005) J Phys Chem A 109:1478–1480
51. Strout DL (2005) J Phys Chem A 108:10911–10916
52. Strout DL (2005) J Chem Theor Comput 1:561–565
53. Politzer P, Murray JS, Grice ME, Sjoberg P (1991) Chemistry of energetic materials. In: Olah GA, Squire DR (eds) Academic, New York
54. Kohler J, Meyer R (1993) Explosives, 4th edn. VCH, Weinheim, Germany
55. Mader CL (1998) Numerical modeling of explosives and propellants. CRC, New York
56. Politzer P, Murray JS (2003) Energetic materials, part 1: decomposition, crystal and molecular properties. Theoretical and Computational Chemistry, Elsevier
57. Hehre WJ, Ditchfield R, Radom L, Pople JA (1970) J Am Chem Soc 92:4796–4801
58. Hehre WJ, Radom L, PvR S, Pople JA (1986) Ab initio molecular orbital theory. Wiley, New York
59. Foresman JB, Frisch A (1996) Exploring chemistry with electronic structure methods, 2nd edn. Gaussian, Pittsburg
60. Li XH, Zhang RZ, Yang XD, Zhang H (2007) J Mol Struct THEOCHEM 815:151–156
61. Williams CI, Whitehead MA (1997) J Mol Struct THEOCHEM 393:9–24
62. Ju XH, Wang X, Bei FL (2005) J Comput Chem 26:1263–1269
63. Wei T, Zhu WH, Zhang XW, Li YF, Xiao HM (2009) J Phys Chem A 113:9404–9412
64. Su XF, Cheng XL, Meng C, Yuan XL (2009) J Hazard Mater 161:551–558
65. Li J, Huang Y, Dong H (2004) Propellants Explos Pyrotech 29:231–235
66. Bulusu S, Damavarapu R, Autera JR, Behrens R, Minier LM Jr, Villanueva J, Jayasuriya K, Axenord T (1995) J Phys Chem 99:5009–5015
67. Agrawal JP (1998) Prog Energy Combust Sci 24:1–30
68. Sikder AK, Sikder N (2004) J Hazard Mater 112:1–15
69. Cho SG, Goh EM, Cho JR, Kim JK (2006) Propellants Explos Pyrotech 31:33–37
70. Licht HH, Ritter H (1997) Propellants Explos Pyrotech 22:333–336
71. Politzer P, Martinez J, Murray JS, Concha MC, Toro-Labbe A (2009) Mol Phys 107:2095–2101
72. Mondal T, Saritha B, Ghanta S, Roy TK, Mahapatra S, Durga Prasad M (2009) J Mol Struct THEOCHEM 897:42–47
73. Cho SG, Goh EM, Kim JK (2001) Bull Korean Chem Soc 22:775–778
74. Minkin VI, Glukhovtsev MN, Simkin BY (1994) Aromaticity and antiaromaticity. Wiley, New York
75. Garratt PJ (1986) Aromaticity. Wiley, New York
76. Eluidge JA, Jackman LM (1961) J Chem Soc 859–866
77. Kamlet MJ, Adolph HG (1979) Propellants Explos Pyrotech 4:30–34
78. Bliss DE, Christian SL, Wilson WS (1991) J Energ Mater 9:319–348